Proceedings of the 2nd International Symposium
on Adaptive Motion of Animals and Machines,
Kyoto, March.4-8, 2003

An Analog CMOS Circuit Implementing CPG Controller for Quadruped Walking Robot

Kazuki NAKADA, Tesuya ASAI and Yoshihito AMEMIYA

[1]Univ. of Hokkaido., Dept. of Electrical Engineering, Sapporo, Hokkaido 060-8628, nakada@sapiens-ei.eng.hokudai.ac.jp

Abstract

In this report, we propose an analog circuit that implements a locomotion controller for a quadruped walking robot. Animal locomotion, such as walking, running, swimming and flying, is based on periodic rhythmic movements driven by the biological neural network, called the central pattern generator (CPG). In recent years, many researchers have applied the CPG to locomotion controller for walking robots. However, most of these have been developed with digital processors, and thus have several problems, such as high power consumption. Hence, we designed an analog CPG controller for the quadruped walking robot. The proposed circuit is based on the Amari-Hopfield model, which is suitable for analog circuit implementation because of its simple transfer function. Since the proposed circuit is constructed from complemental metal-oxide semiconductor (CMOS) devices, which operate in their subthreshold region, it can reduce power consumption. By computer simulations, the proposed circuit is shown to have the capability to generate several periodic rhythmic patterns and transitions between their patterns promptly.

1. Introduction

Animal locomotion, such as walking, running, swimming and flying, is based on periodic rhythmic movements. These rhythmic movements are driven by the biological neural network, called the central pattern generator (CPG). The CPG consists of sets of neural oscillators, situated in ganglion or spinal cord. Induced by tonic inputs from command neurons, the CPG generates a rhythmic pattern of neural activity unconsciously and automatically. As a result of such a rhythmic pattern activating the motor neurons, the rhythmic movements of animals are driven. [1]. While not necessary for generating rhythmic movements, sensory feedback regulates the frequency and phase of these rhythmic patterns generated by the CPG [2]. Furthermore, the CPG can adapt to various environments to change the periodic rhythmic pattern itself. For instance, vertebrates, such as horses and cats, can change their locomotor patterns depending on the situation [3]. Since the coordination of physical parts is required for smooth locomotion, the rhythmic movements driven by the CPG play one of the most important roles in locomotion.

In recent years, many researchers have applied the CPG to locomotion controllers for quadruped walking robots [9]-[12]. For example, quadruped robots capable of adaptating to irregular terrain using CPG dynamics have been developed by Kimura *et. al* [9]. Ijspeert and Billard have applied the CPG to control of an entertainment robot, AIBO [10].

In robotics, using the CPG for locomotion control has the following advantages: i) The amount of calculation required for movement control is reduced as a result of the coordination of physical parts induced by the rhythmic movements, ii) As a result of synaptic plasticity changing the substantial structure of the CPG and the rhythmic pattern, high autonomous adaptation to various environments is achieved.

In this report, we propose an analog CPG controller to coordinate of physical parts for quadruped walking robots. Although a number of the CPG controllers have been developed, most of these are implemented by using digital processors [8]-[10]. While the digital processor can operate with high accuracy, it consumes high power and requires a large area of a chip. Such problems degrade the CPG controller. In order to improve such problems, the proposed circuit is designed as an analog circuit. Since the proposed circuit operates in the subthreshold region, it can reduce power consumption. By computer simulations, we confirm the operation of the proposed circuit.

2. The Role of The CPG Control

The rhythmic movements of animals, such as locomotion and breathing, are driven by the CPG. The CPG generates a periodic rhythmic pattern of neural activity that activates motor neurons, resulting in the rhythmic movements of animals. The periodic rhythmic pattern of neural activity can be regarded as an attractor like

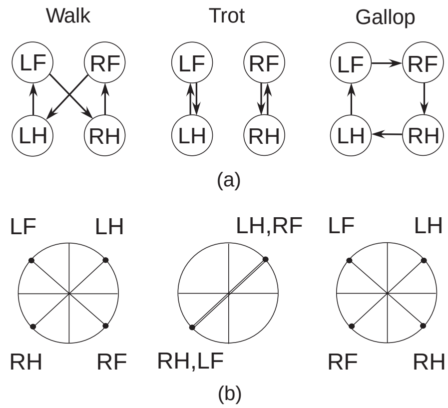

Figure 1: (a) The typical gait patterns in quadruped locomotion. (b) The relative phases of each limbs in the different gait patterns, where LF,LH,RF and RH are left forelimb, left hindlimb, right forelimb and right hindlimb respectively.

a limit cycle, embedded in the CPG network structure. Characteristics of the rhythmic pattern as an attractor contribute to the stability of the rhythmic movements.

In vertebrate locomotion, one of the most fundamental roles of the CPG is to control each limb. As a result of the interaction with the CPGs that actuate each of the joints, the rhythmic movements of each limb are stabilized. Another role is cooperation between the limbs, i.e., interlimb coordination. CPGs that control each of the limbs are synchronized via coordinating interneuros between the CPGs, and thus the interlimb coordination is achieved. Since the degree of the freedom of physical parts relevant to locomotion is very high, the coordination of physical parts is required for smooth locomotion. Therefore, CPG can be said to play the central role in locomotion.

In the locomotion of mammals, transitions of the rhythmic movements are often observed. As a typical example, the horse has chosen a locomotor pattern called the gait. It is believed that optimal gait pattern is chosen based on locomotor speed or the rate of energy consumption [3]. Such a transition of rhythmic movements is also controlled by the CPG. In addition, each of the gait patterns, such as walk, trot and gallop, is characterized by the relative phase between the limbs (Fig. 1). It is considered that the transitions of the rhythmic movements are performed as a result of the regulation of the relative phase by the CPG. Recently, it has been considered that the substantial network structure of the CPG is changed due to modulation in the synaptic strength caused by a neuromodulator. Hence it follows that the coordination of physical parts is also changed

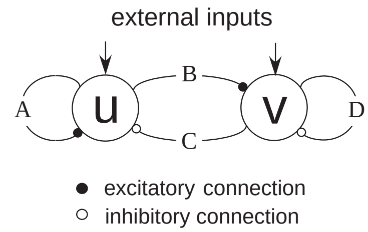

Figure 2: The configuration of the Amari-Hopfield model.

3. The CPG model

3.1. Neural Oscillator Model

A number of artificial neural networks have been proposed as the CPG model [4]-[6]. In the earliest research, Brown proposed the most fundamental CPG model using the neural oscillator, which consists of two neurons and has interactions between neurons by reciprocal inhibition [4]. Although its configuration is very simple, it is essential as the component of the CPG model.

In the present work, we chose the Amari-Hopfield model [7] as the neural oscillator. The model consists of an excitatory neuron and an inhibitory neuron with excitatory inhibitory connections (Fig. 2). The dynamics of the model is expressed by the following equations:

$$\begin{cases} \tau\dot{u} = -u + A{\cdot}f_\mu(u) - C{\cdot}f_\mu(v) + S_u(t) \\ \tau\dot{v} = -v + B{\cdot}f_\mu(u) - D{\cdot}f_\mu(v) + S_v(t) \end{cases} \quad (1)$$

where u and v express the activities of the excitatory neurons and the inhibitory neurons, respectively. The parameters A, B, C and D determine the dynamics of the model. $S_u(t)$ and $S_v(t)$ express the external inputs. The transfer function $f_\mu(x)$ is given by the following equation:

$$f_\mu(x) = \frac{1 + \tanh(\mu x)}{2} \quad (2)$$

where $\tanh(x)$ is the hyperbolic tangent function and μ is its control parameter. The Amari-Hopfield model is suitable for implementation of the CPG model as analog circuits because of its simple transfer function. Its details are given in the following section. The dynamics of the model has been studied in detail. Depending on the parameters A through D and the external inputs $S_u(t)$ and $S_v(t)$, the Amari-Hopfield model generates the periodic pattern automatically.

3.2. Neural Network Model

We composed a neural network model as the CPG controller to perform interlimb coordination. As the CPG controller for interlimb coordination, it is desirable to generate various rhythmic patterns. Hence, we constructed a neural network model from the Amari-Hopfield model according to the CPG model proposed by Nagashino *et. al* [14]. Their model consists of four coupled neural oscillators with reciprocal inhibition, and excitatory and inhibitory interneurons are introduced. As a result of introducing the interneurons and controlling their interactions with neural oscillators, substantial network structure is changed and various rhythmic patterns are generated [14].

Figure 3 shows the basic structure of the neural network model. Here, we describe configurations of networks that generate periodic rhythmic patterns corresponding to each of the typical gaits of mammals. Figures 4(a)-(c) correspond to the walk mode, the trot mode and the gallop mode, respectively.

By combining the networks that correspond to each of the gait modes, the entire network is constructed. The network dynamics are given by the following equations:

$$\begin{aligned}\tau_u \dot{u}^{\{0,1,2,3\}} &= -u^{\{0,1,2,3\}} + A f_\mu(u^{\{0,1,2,3\}}) \\ &+A_w f_\mu(u_w^{\{2,3,1,0\}}) + A_g f_\mu(u_g^{\{2,0,3,1\}}) \\ &-C_{lr} f_\mu(v^{\{1,0,3,2\}}) - C_{fh} f_\mu(v^{\{2,3,0,1\}}) \\ &-C f_\mu(v^{\{0,1,2,3\}}) + I_u^{\{0,1,2,3\}}(t) \end{aligned} \tag{3}$$

$$\begin{aligned}\tau_v \dot{v}^{\{0,1,2,3\}} &= -v^{\{0,1,2,3\}} + B f_\mu(u^{\{0,1,2,3\}}) \\ &-D_t f_\mu(v_t^{\{3,2,1,0\}}) + I_v^{\{0,1,2,3\}}(t) \end{aligned} \tag{4}$$

$$\begin{aligned}\tau_w \dot{u}_w^{\{0,1,2,3\}} &= -u_w^{\{0,1,2,3\}} + A_w f_\mu(u^{\{0,1,2,3\}}) \\ &+I_{uw}^{\{0,1,2,3\}}(t) \end{aligned} \tag{5}$$

$$\begin{aligned}\tau_g \dot{u}_g^{\{0,1,2,3\}} &= -u_g^{\{0,1,2,3\}} + A_g f_\mu(u^{\{0,1,2,3\}}) \\ &+I_{ug}^{\{0,1,2,3\}}(t) + I_{xg}^{\{0,1,2,3\}}(t) \end{aligned} \tag{6}$$

$$\begin{aligned}\tau_t \dot{v}_t^{\{0,1,2,3\}} &= -v_t^{\{0,1,2,3\}} - D_t f_\mu(v^{\{0,1,2,3\}}) \\ &+I_{vt}^{\{0,1,2,3\}}(t) + I_{xt}^{\{0,1,2,3\}}(t) \end{aligned} \tag{7}$$

where the numbers correspond to each unit, u, u_w and u_g represent activities of the excitatory neurons, v and v_t represent activities of the inhibitory neurons, τ_u, τ_v, τ_{u_w}, τ_{u_g} and τ_{v_t} are the time constant of the neurons, A, A_w, A_g, B, C, C_{lr}, C_{fh} and D_t are the interaction parameters, I_u, I_v, I_{u_w}, I_{u_g} and I_{v_t} are the tonic bias inputs and $I_{x_t}^{\{k\}}$ $(k = 0, 1, 2, 3)$ are the external inputs to the interneurons.

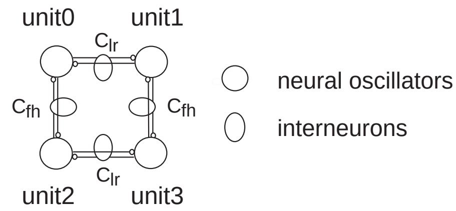

Figure 3: The basic configuration of the network.

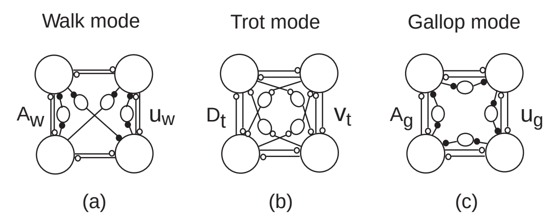

Figure 4: The configurations of the networks correspond to the typical gait patterns. (a) The walk mode. (b) The trot mode. (c) The gallop mode.

4. The CPG Controller

In this section, the neural oscillator circuit underlying the CPG controller is described, and we construct the CPG controller from the neural oscillator circuit.

4.1. Neural Oscillator Circuit

First, we describe the characteristics of the differential pair, which is one of the most fundamental components of the neural oscillator circuit. The differential pair can approximate the transfer function. When the MOS transistors, which comprise the differential pair, operate in their subthreshold region, the static response of the differential pair is given by the following equation [15]:

$$I_\mu(v) = I_b \frac{1 + \tanh(\mu(v - v_b))}{2} \tag{8}$$

where v is the input voltage, v_b is the bias voltage, $\mu = \kappa/2V_T$, V_T is the thermal voltage, I_b is the bias current and κ is the device parameter.

The excitatory cell circuit is shown in Fig. 5. It consists of the CR circuit, the differential pair and the current source. The dynamics of the excitatory cell is given by the following equation:

$$C_u \dot{u} = -\frac{u}{R_u} + I_u(t) \tag{9}$$

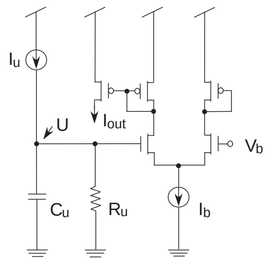

Figure 5: The schematic of the excitatory circuit.

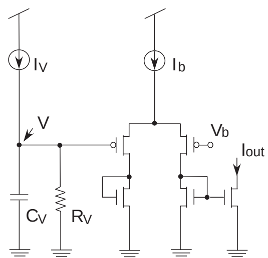

Figure 6: The schematic of the excitatory circuit.

where u expresses the voltage value, C_u is the capacitance value, R_u is the resistance value and $I_u(t)$ is the external current. The excitatory cell outputs positive current according to (8).

The inhibitory cell circuit is shown in Fig. 6. It also consists of the CR circuit, the differential pair and the current source. The dynamics of the inhibitory cell is given by the following equation:

$$C_v \dot{v} = -\frac{v}{R_v} + I_v(t) \tag{10}$$

where v expresses the voltage value, C_v is the capacitance value, R_v is the resistance value and $I_v(t)$ is the external current. The inhibitory cell outputs negative current according to (8).

The neural oscillator circuit is constructed from the excitatory circuit and the inhibitory circuit (Fig. 7), and its dynamics is given by rewriting (1) as follows:

$$\begin{cases} C_u \dot{u} = -\dfrac{u}{R_u} + A \cdot I_\mu(u) - C \cdot I_\mu(v) + I_u(t) \\ C_v \dot{v} = -\dfrac{v}{R_v} + B \cdot I_\mu(u) + I_v(t) \end{cases} \tag{11}$$

where the parameters A through C are the same as in (1), and $I_\mu(u)$ and $I_\mu(v)$ are the output currents of the differential pairs. The circuit generates periodic rhythmic patterns, depending on the parameters A through C and the external inputs $I_u(t)$ and $I_v(t)$.

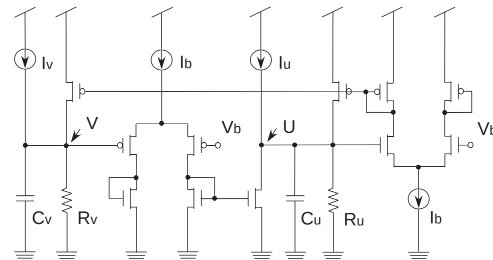

Figure 7: The schematic of the neural oscillator circuit.

4.2. The Network Circuit

We constructed the CPG network circuit from the neural oscillator circuit. Here, we use the excitatory cell as the excitatory interneurons and the inhibitory cell as the inhibitory interneuros. Let us rewrite (3)-(7) as follows:

$$\begin{aligned} C_u \dot{u}^{\{0,1,2,3\}} &= -\frac{u^{\{0,1,2,3\}}}{Ru} + A I_\mu(u^{\{0,1,2,3\}}) \\ &+ A_w I_\mu(u_w^{\{2,3,1,0\}}) + A_g I_\mu(u_g^{\{2,0,3,1\}}) \\ &- C_{lr} I_\mu(v^{\{1,0,3,2\}}) - C_{fh} I_\mu(v^{\{2,3,0,1\}}) \\ &- C I_\mu(v^{\{0,1,2,3\}}) + I_u^{\{0,1,2,3\}} \end{aligned} \tag{12}$$

$$\begin{aligned} C_v \dot{v}^{\{0,1,2,3\}} &= -\frac{v^{\{0,1,2,3\}}}{Rv} + B I_\mu(v^{\{0,1,2,3\}}) \\ &- D_t I_\mu(v_t^{\{3,2,1,0\}}) + I_v^{\{0,1,2,3\}} \end{aligned} \tag{13}$$

$$\begin{aligned} C_w \dot{u}_w^{\{0,1,2,3\}} &= -\frac{u_w^{\{0,1,2,3\}}}{Ru_w} + A_w I_\mu(u^{\{0,1,2,3\}}) \\ &+ I_{uw}^{\{0,1,2,3\}} \end{aligned} \tag{14}$$

$$\begin{aligned} C_g \dot{u}_g^{\{0,1,2,3\}} &= -\frac{u_g^{\{0,1,2,3\}}}{Ru_g} + A_g I_\mu(u^{\{0,1,2,3\}}) \\ &+ I_{ug}^{\{0,1,2,3\}} \end{aligned} \tag{15}$$

$$\begin{aligned} C_t \dot{v}_t^{\{0,1,2,3\}} &= -\frac{v_t^{\{0,1,2,3\}}}{Rv_t} - D_t I_\mu(v^{\{0,1,2,3\}}) \\ &+ I_{vt}^{\{0,1,2,3\}} + I_{xt}^{\{0,1,2,3\}} \end{aligned} \tag{16}$$

where $I_\mu(\cdot)$ is the output current of the differential pair. The capacitance values C_u through C_{vt}, the resistance values R_u through R_{vt}, and the interaction parameters A through D_t correspond to those in equations (3)-(7). I_u, I_v, I_{uw}, I_{ug}, I_{vt} and I_{xt} are the DC bias currents. The ratio of the interaction parameters is determined by the aspect ratio W/L (W: the gate width, L: the gate length) of the transistors, which comprise the current mirrors in the circuits. These values are determined by the bias currents of the differential pairs. Depending on interaction parameters A through D_t, the rhythmic pattern corresponding to each gait pattern is generated.

5. Results

In this section, we confirm the operation of the proposed circuit by computer simulation. In the following simulation, we used the circuit simulator PSPICE and assumed 1.5-μm CMOS device technology. As typical device parameters, I_0=$O(10^{-16})$ A and $\kappa = 0.6$ are assumed. As common parameters, the gate length L=1.5μm, the capacitance values C_u, C_v, C_{ug}, C_{vt} and C_{uw} were set at (100, 100, 100, 100, 300) nF, the resistance values $R_u, R_v, R_{u_w}, R_{u_g}$ and R_{v_t} were set at 1 MΩ, the interaction parameters A, B, C, C_{lr} and C_{fh} set as follows:

$$A = C = 4.0,\ B = 3.0,\ C_{lr} = C_{fh} = 1.0$$

where we set the bias currents of the differential pairs at 100 nA.

5.1. Production of Multiple Gait Patterns

First, we confirmed the generation of the periodic rhythmic patterns in the circuit. Three examples of the rhythmic pattern generated by the circuit are shown in Figs. 8(a)-8(c). It is shown that each periodic rhythmic pattern corresponds to the typical gait patterns.

Figure 8(a) corresponds to the walk mode. In the mode, we set the parameters as follows:

$$A_w = 2.0,\ A_g = D_t = 0.0$$

The bias currents I_u, I_v, I_{uw}, I_{ug} and I_{vt} were set at (0.95, 0.85, 0.85, 1.0, 1.0) μA, the bias currents $I_{xt}^{\{k\}}$ were set at 0 A $(k = 0, 1, 2, 3)$.

Figure 8(b) corresponds to the trot mode. In the mode, we set the parameters at as follows:

$$D_t = 1.0,\ A_w = A_g = 0.0$$

The bias currents I_u, I_v, I_{uw}, I_{ug}, and I_{vt} were set at (1.1, 0.9, 1.0, 1.0, 1.05) μA, the bias currents $I_{xt}^{\{0\}}$ $I_{xt}^{\{1\}}$, $I_{xt}^{\{2\}}$ and $I_{xt}^{\{3\}}$ were set at (2, 0, 0, 2) nA.

Figure 8(c) corresponds to the gallop mode. In the mode, we set the parameters at as follows:

$$A_g = 3.0,\ A_w = D_t = 0.0$$

The bias currents I_u, I_v, I_{uw}, I_{ug} and I_{vt} were set at (1.0, 0.85, 1.0, 0.9, 1.0) μA, the bias currents $I_{xt}^{\{k\}}$ were set at 0 A $(k = 0, 1, 2, 3)$.

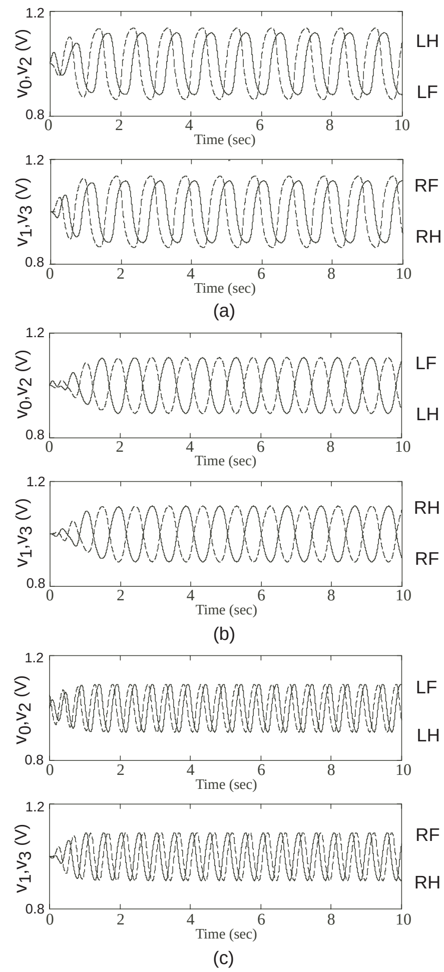

Figure 8: The waveforms correspond to the gait patterns. (a) The walk mode. (b) The trot mode. (c) The gallop mode.

5.2. Gait Pattern Transitions

Second, we confirmed the transitions between the different patterns in the circuit. In the following simulation, the interaction parameters and the bias currents were changed at 5.0 (s). Figures 9(a) and (b) show examples of transitions in the circuit. These Figures correspond to the transition from walk to trot and from trot to gallop, respectively. In each mode, it is shown that the circuit has the capability to change the rhythmic patterns promptly.

As a result of several computer simulations, we confirmed the performance of the proposed circuit. First, we confirmed that the circuit has the capability of generating some rhythmic periodic patterns correspond to the gait patterns. Second, we confirmed the transitions from one pattern to another.

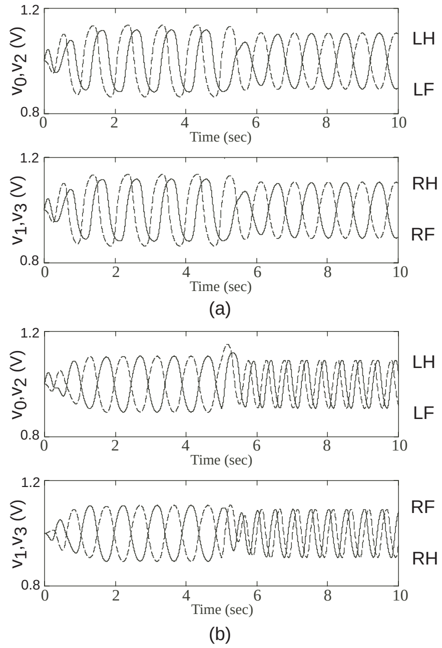

Figure 9: The transitions between the different modes.

6. Conclusion

In this paper, we proposed an analog CPG controller for a quadruped walking robot. In recent years, many researchers have implemented the CPG controllers in robotics. However, most of these have been developed with digital processors, and thus have such problems as high power consumption. Hence, we designed the CPG controller as analog circuit. In previous works, some analog CPG controllers have already been developed [11]-[13]. For instance, Lewis *et. al*, proposed custom an analog VLSI chip as a CPG controller, which makes use of the integrated and fire neurons [12]. Still *et. al* created a quadruped walking machine using an analog CPG controller based on the Morris-Lecar neurons [13]. The present work differs from the previous works in several respects. First, the CPG controller is based on the Amari-Hopfield neuron, which is easily implemented by using fundamental analog circuits. Second, the proposed CPG controller has the capability to produce various rhythmic patterns and transitions between the periodic rhythmic patterns promptly. Since the proposed circuit is constructed from the CMOS transistors, which operate in their subthreshold region, it can reduce power consumption. Moreover, it has achieved low-cost and a small area of a chip. These characteristics are sufficient as the CPG controller. Following the present research, we will be aiming to develop micro locomotor robots.

References

[1] F. Delcomyn, *Foundations of Neurobiology*, W.H. Freeman and Co, New York, 1997.

[2] *The Handbook of Brain Theory and Neural Networks, Second Edition*.M. Arbib Ed., USA, MIT PRESS, Press 2002.

[3] J. Nishii, ”Legged animals select the optimal locomotor pattern based on energetic cost,” *Biological Cybernetics*., vol.83, pp.435-442, 2000.

[4] G. Brown. ”On the nature of the fundamental activity of the nearvous centers;together with an anlysis of the conditioning of the rhythmic activity in progression, and a theory of the evoution of function in the nervous system,” *J. Physiol.*, vol 48,pp.18-46, 1914.

[5] K. Matsuoka, ”Mechanism of Frequency and Pattern Control in the Neural Rhythm Generators,” *Biological Cybernetics*., vol,56, pp.345-353, 1987.

[6] G. Taga, Y. Yamaguchi and H. Shimizu, ”Self-organaized control of bipedal locomotion by neural oscillators in unpredictable environment,” *Biological Cybernetics*., vol. 65, pp.147-159, 1991.

[7] S. Amari, ”Characteristic of the random nets of analog neuron-like elements,” *IEEE trans. on System, Man and Cybernetics*, SMC-2, pp.643-657, 1972.

[8] J. Shan, F. Nagashima, ”Neural Locomotion Controller Design and Implementation for Humanoid Robot HOAP-1”, In *proc. The 20th RSJ conference*, 2002.

[9] H. Kimura, Y. Fukuoka and K. Konaga, ”Adaptive Dynamic Walking of a Quadruped Robot by Using Neural System Model,” *ADVANCED ROBOTICS*, Vol.15, No.8Cpp.859-876, 2001.

[10] A. J. Ijspeert and A. Billard, ”Biologically inspired neural controllers for motor control in a quadruped robot,” In *proc, International Joint Conference on Neural Network conference.*, 2000.

[11] G. Patel, J. Hollemam and S. Deweerth, ”Analog VLSI Model of Intersegmental Coordination with Nearest Neighbor Coupling,” In *Adv. Neural Information Processing*., vol. 10, pp.710-725, 1998.

[12] M. A. Lewis, M. J. Hartmann, R. Etienne-Cummings, A. H. Cohen, ”Control of a robot leg with an adaptive aVLSI CPG chip”, *Neurocomputing*., vol.38-40, pp 1409-1421, 2001.

[13] S. Still and M. W. Tilden, ”Controller for a four legged walking machine, In:Neuromorphic Systems:Engineering Silicon from Neurobiology, Eds:. S. Smith and A. Hamilton,” *World Scientific*., Singapore, pp.138-148, 1998.

[14] H.Nagashino, Y. Nomura and Y. Kinouchi. ”Generation and Transitions of Phase-Locked Oscillations in Coupled Neural Oscillators”, In *proc, The fortieth SICE Annual Conference*, 2001.

[15] C. A. Mead, *Analog VLSI and Neural Systems*, Reading, Mass, Addison-Wesley, 1989.